Discovery of widely available abyssal rock patches reveals overlooked habitat type and prompts rethinking deep-sea biodiversity

Torben Riehl[a,b,1], Anne-Cathrin Wölfl[c], Nico Augustin[c], Colin W. Devey[c], and Angelika Brandt[a,b]

[a]Department of Marine Zoology, Section Crustacea, Senckenberg Research Institute, 60325 Frankfurt, Germany; [b]Institute for Ecology, Diversity and Evolution, Goethe University Frankfurt, 60439 Frankfurt am Main, Germany; and [c]Research group Dynamics of the Ocean Floor, GEOMAR Helmholtz Centre for Ocean Research Kiel, 24148 Kiel, Germany

Edited by Steven M. Stanley, University of Hawaii, Honolulu, HI, and approved May 8, 2020 (received for review November 24, 2019)

Habitat heterogeneity and species diversity are often linked. On the deep seafloor, sediment variability and hard-substrate availability influence geographic patterns of species richness and turnover. The assumption of a generally homogeneous, sedimented abyssal seafloor is at odds with the fact that the faunal diversity in some abyssal regions exceeds that of shallow-water environments. Here we show, using a ground-truthed analysis of multibeam sonar data, that the deep seafloor may be much rockier than previously assumed. A combination of bathymetry data, ruggedness, and backscatter from a trans-Atlantic corridor along the Vema Fracture Zone, covering crustal ages from 0 to 100 Ma, show rock exposures occurring at all crustal ages. Extrapolating to the whole Atlantic, over 260,000 km^2 of rock habitats potentially occur along Atlantic fracture zones alone, significantly increasing our knowledge about abyssal habitat heterogeneity. This implies that sampling campaigns need to be considerably more sophisticated than at present to capture the full deep-sea habitat heterogeneity and biodiversity.

hydroacoustics | remote sensing | geobiodiversity | habitat mapping | polymetallic nodules

One of the major knowledge gaps in marine ecology and biogeography is the understanding of the processes responsible for the evolution and persistence of biodiversity on the deep seafloor, as well as determining the significant scales of these processes. Abyssal seafloor, between 3,501 and 6,500 m depth, covers 65–75% of the ocean floor (1, 2). Gross continuity and homogeneity in physical environmental parameters characterize the abyss even taking into account that seafloor features are meanwhile known to occur widely scattered across ocean basins, such as volcanic ridges, seamounts, and plateaus. The generally level (relief <300 m) and unstructured abyssal plains, often described as sediment-covered landscapes, border the continental slopes and subduction zones (3, 4). They dominate the abyssal depth zone and make up 33.2% of the ocean floor (5). Abyssal sedimentation rates are assumed to be generally low and constant over large areas (6). As crust ages with distance from the spreading axis, the accumulation of sediment generally increases (7, 8). The global map of total sediment thickness [US National Oceanic and Atmospheric Administration (9)] suggests that—apart from midocean ridges—the entire abyssal seafloor is covered by sediments up to hundreds of meters thick. Even in areas that today are exposed to minimal sedimentation rates, a sediment layer of several meters thickness is assumed (10–12).

This picture of a mainly flat, sedimented seafloor seems at odds with biological observations. Strong links between habitat diversity and organismal species richness have been shown in many ecosystems including, more recently, in the abyss (13–18). In a suite of various (partially interacting) factors, like energy availability (19), temperature (20), and disturbance (21), habitat heterogeneity is a driver for community variation and biodiversity in the deep-sea benthic environment (22) as well as for geographic patterns of diversity (23). It influences, for example, resource partitioning, predation, competitive exclusion, and connectivity but under the assumption of a homogeneous abyssal seafloor, habitat heterogeneity may be underappreciated as a factor in abyssal biodiversity studies. Much may be gained from considering it because theoretical models predict environmental heterogeneity and habitat boundaries positively affect diversification (24, 25) and thus the evolution of biodiversity. Separate habitat patches with their inherent boundaries allow for separation of subpopulations, and provide opportunities for adaptive radiation. The abyss exhibits high species richness and the abyssal fauna often comprise many hundreds of macrofaunal and megafaunal species on the scale of a few square kilometers; the figure for the meiofauna is even larger (e.g., refs. 26–29). A few recent studies have begun to investigate deep-sea habitat diversity using a combination of high-resolution hydroacoustic measurements, photo and video observations, as well as seafloor

Significance

Ground-truthed analyses of multibeam sonar data along a fracture zone of the northern Mid-Atlantic Ridge reveal an abyssal seafloor much rockier than previously assumed. Our data show rock exposures occurring at all crustal ages from 0–100 Ma along the Vema Fracture Zone and that approximately 260,000 km^2 of rock habitats can be expected to occur along Atlantic fracture zones alone. This higher than expected geodiversity implies that future sampling campaigns should be considerably more sophisticated than at present to capture the full deep-sea habitat heterogeneity. We provide a baseline to unravel the processes responsible for the evolution and persistence of biodiversity on the deep seafloor as well as to determine the significant scales of these processes in the benthoscape.

Author contributions: T.R. designed research; T.R., A.-C.W., and N.A. performed research; A.-C.W., N.A., and C.W.D. contributed new reagents/analytic tools; A.-C.W. and N.A. analyzed data; T.R., A.-C.W., N.A., C.W.D., and A.B. wrote the paper; T.R., A.-C.W., and N.A. provided critical feedback and helped shape the research and manuscript; C.W.D. had impact on the study design by providing thoughts and ideas and initiated the study with their successful ship-time application, provided critical feedback, and helped shape the research and manuscript, proofreading the manuscript for quality of the English; and A.B. had impact on the study design by providing thoughts and ideas and initiated the study with their successful ship-time application, provided critical feedback, and helped shape the research and manuscript.

The authors declare no competing interest.

This article is a PNAS Direct Submission.

Data deposition: The bathymetric dataset has been made available on PANGAEA (https://doi.pangaea.de/10.1594/PANGAEA.893352).

[1]To whom correspondence may be addressed. Email: triehl@senckenberg.de.

This article contains supporting information online at https://www.pnas.org/lookup/suppl/doi:10.1073/pnas.1920706117/-/DCSupplemental.

sampling (17, 30–32). Data from the lower bathyal at the northern Mid-Atlantic Ridge show a relationship between slope angle and sediment coverage where moderate slopes are characterized by occasional rock outcrops while steep slopes are dominated by bare rock surfaces (30, 33). In such studies, hard substrates have been identified as promoters of habitat heterogeneity and diversity (34), and they highlight that hard substrates are required for sessile deep-sea fauna such as many Bryozoa, Porifera, or Cnidaria (30). Nevertheless, the distribution of exposed rock in the abyss and its effects on habitat heterogeneity has not yet been studied.

The Atlantic abyssal region is cross-cut by many "fracture zones"—intraplate traces of active plate-boundary faults at the spreading axis. We have previously presented geological data from several biological sampling sites within one such zone, the Vema Fracture Zone (VFZ), producing high-resolution habitat maps for the interpretation of species distribution data in several regions of interest (31). These maps of distinct sites showed exposed rock and an overall higher than expected heterogeneity comprising varying slope angles at various sizes and spatial coverage. Here we expand this analysis to the whole fracture zone (crustal ages covered roughly 0–100 Ma), characterizing the seafloor and quantifying habitat types based on the combination of two sonar-related indices and ground-truthed with seafloor sampling. The VFZ data are then extrapolated over the totality of the many Atlantic fracture zones. This allows us to estimate the amount of sediment-free seafloor which may be present in the Atlantic. Our finding suggest that "hard rock" should be added to the list of currently 17–25 (depending on author) habitat types recognized in the abyss (1, 35) and that previous explanations for biodiversity patterns in the abyss may need to be rethought. This approach is an initial step toward using hydroacoustic remote sensing as a mapping tool for habitat and biodiversity assessments in the framework of effective conservation strategies and sustainable exploitation in the abyss.

Results

Seafloor Characterization in the VFZ. Almost 95,000 km^2 of seafloor in the VFZ (Fig. 1 and *SI Appendix*, Fig. S1) was surveyed using a ship-mounted multibeam echosounder, providing information on both seafloor relief and acoustic backscatter (Table 1). In total, 8,289 km^2 (9%) of the seafloor was characterized as having high hard-rock exposure potential. In particular the neovolcanic zone at the Mid-Atlantic Ridge comprised a large proportion of high hard-rock exposure potential (Fig. 2). Regions showing a moderate hard-rock exposure potential comprised 31,194 km^2 (33%). The moderate backscatter values combined with medium and high ruggedness index (RI) values in these regions indicate a patchy distribution of hard seafloor within sedimented areas.

Geologically, such areas of medium hard-rock exposure potential are characterized by volcanic ridges and steep valley flanks (Fig. 2 and *SI Appendix*, Fig. S2). In addition, areas with low relief but where polymetallic nodules have been sampled (Figs. 3 and 4 and *SI Appendix*, Table S1) also fall in this category due to the higher backscatter (BS) response of the seafloor. The remaining low-RI–low-BS regions, which have a low hard-rock exposure potential, account for the largest proportion of seafloor within the survey area covering 54,925 km^2 (58%).

Interpretation of the acoustic data was confirmed by seafloor sampling and photography (37) using dredges, grabs, gravity corers, a camera-equipped epibenthic sledge [C-EBS (38)], and an autonomous underwater vehicle (AUV; Figs. 3 and 4 and *SI Appendix*, Table S1).

Surface-Area Estimation of Exposed Hard Rock in Atlantic Fracture Zones. The abyssal fracture zones of the Atlantic Ocean (Fig. 5) are estimated to cover 92,709 km^2 of young crust (0–5 Ma), 1,583,55 km^2 of medium old (5–50 Ma) crust, and 1,237,175 km^2 of old (50–100 Ma) crust (Table 2). Our own survey did not cover areas much older than 100 Ma and hence, older crust was not considered in this paper.

In the young VFZ (0–5 Ma), 30% of the seafloor had a high hard-rock exposure potential. Based thereupon our estimation of total available hard rock in Atlantic fracture zones is 27,813 km^2. Taking into account also the two additional age classes medium (11%; 174,191 km^2) and old (5%; 61,859 km^2), a total area of 263,863 km^2 is estimated for this habitat type across Atlantic fracture zones (Table 2).

Discussion

Our study provides a crude estimation for the availability of hard-rock surfaces at abyssal depths in Atlantic fracture zones. Using multibeam echosounder data, submarine features along the VFZ were revealed in detail. High-resolution bathymetry, BS data, and terrain analyses provided a detailed impression of seafloor characteristics and allowed hard-substrate discovery and quantification. It showed that, depending on the study region, up to 30% of the mapped seafloor comprises exposed hard rock representing habitats for benthos dependent on hard substrate. This has profound implications on the variability and fragmentation of abyssal habitats—important factors for the formation and persistence of biodiversity on the deep seafloor.

Less than 10% of the seafloor has ever been surveyed by multibeam sonar (39)—the only information about its possible shape over the remaining 90% was derived from modeling of satellite gravimetric data. Nevertheless, such data have been used to generate habitat maps of the whole seafloor (5). The data we present here originated from areas classified as "abyssal hill" and "abyssal mountains" in such maps (5). We find that both flat soft-sediment plains and slopes with exposed hard rock occur in both categories, highlighting that low-resolution gravimetric data are insufficient for habitat differentiation. Direct observations from ship-based echosounder data and ground-truthing with seafloor sampling is essential for differentiation between habitat types.

In our analysis, a high potential to encounter hard seafloor was mainly found at and proximal to the Mid-Atlantic Ridge (Fig. 2 and Table 2). This is unsurprising as the young oceanic lithosphere (0–5 Ma) there has little sediment covering. The proportion of hard-rock exposure potential decreases with crustal age and therefore increasing distance to the ridge axis. Far from the ridge, the distribution was spatially widely scattered and patchy. However, at medium crustal ages (5–50 Ma) a significant proportion of area with high hard-rock exposure potential was detected. On very old crust (50–100 Ma) the potential for exposed hard rock was lowest, but with local and regional variation which can be explained by differences in the underlying seafloor topography (Fig. 2 and Table 2).

Seafloor sampling particularly at the station #9–2 shows that the categories A2 (medium BS, low RI) and A3 (high BS, low RI), but also B1–B2 (medium RI, low–medium BS) already indicate hard substrate. The classification at this successful sampling site (Fig. 3) resulted in a complex patchwork of seafloor types including the categories A1–A3, B1, and B2. This habitat diversity is reflected in the seafloor images taken at this site (Fig. 4 *E*, *G*, and *H*) and sampling (*SI Appendix*, Table S1) featuring sediment plains, nodule fields, and manganese-encrusted rock. Thus principally our interpretation of the hydroacoustic data could be confirmed although due to the sampling methods available during that cruise an exact validation of each habitat type has not been possible.

The inferential consequence is that the values provided from RI on the one hand, and BS on the other, cannot be seen as reciprocally interchangeable or necessarily supporting each other but rather as complementary. Accordingly, the combination of the provided values rather than the separate indices converges to a realistic picture of available hard substrate in the abyss.

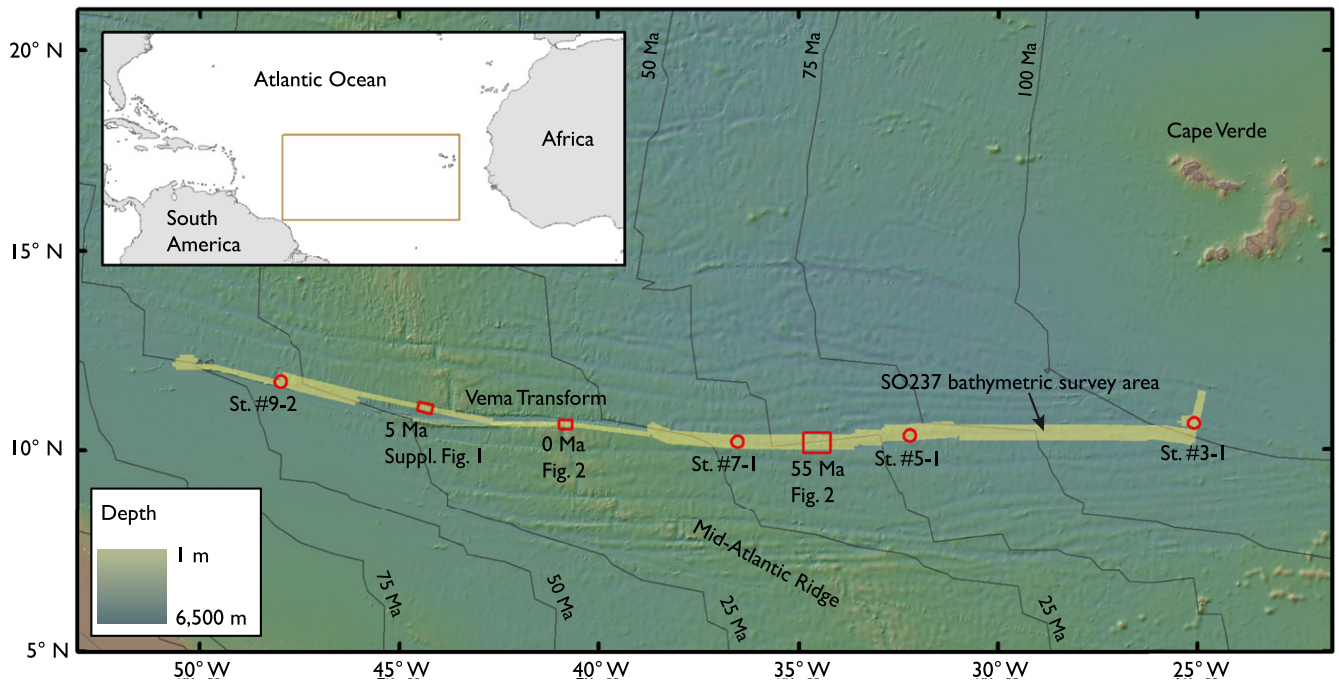

Fig. 1. Study area. Extent of the Vema-TRANSIT high-resolution bathymetry collected in the VFZ (North Atlantic) during cruise SO237. Areas highlighted as rectangles are depicted in Fig. 2 and *SI Appendix*, Fig. S2. Areas highlighted with circles (annotated with station numbers) indicate where rock samples were collected (*SI Appendix*, Table S1). Lithospheric ages were assigned to each station based on the 6-min-resolution age grid of Müller et al. (36).

Implications for Explaining Abyssal Biodiversity. Habitat heterogeneity has been hypothesized to trigger multiple and cascading diversity effects through ecological assemblages (40). While turnover in major habitat types may promote genetic isolation leading to speciation on regional scales, microscale variation in factors such as sediment type and topography may contribute to local coexistence of species (40). On this background it can be assumed that biodiversity regulation through rock surfaces occurs in various ways: primarily through offering attachment sites for sessile organisms, caves, and crevices; secondarily by providing a range of exposures to currents transporting food particles and larvae; thirdly, seafloor topography prompts shear and hence variations in near-seafloor currents, leading to sediment sorting and variation in particle size and food availability (30); finally, rocky outcrop contributes to environmental patchiness, creating barriers to connectivity for some organisms between (semi) isolated abyssal sediment habitats promoting diversification (24, 25). Wherever a variation of slope angle occurs, temporal variability of sediment accumulation and redistribution through slumping may furthermore increase habitat diversity.

Where hard substrate is available in the abyss, the taxonomic composition of the benthic fauna has been found to significantly differ from adjacent sediments. In manganese nodule fields, for instance, sessile suspension-feeding sponges, cnidarians, and Foraminifera were among the dominant taxa which is uncommon for other abyssal habitats (34, 41). The availability of manganese nodules as hard substrate has been shown to drive megafaunal diversity (17, 42). This may also apply to other types of hard substrates in the abyss. Our analysis suggests that species dependent on hard substrates may have much more habitat available than previously assumed. If our observations from the VFZ can be generalized and our estimations for the Atlantic (Fig. 5) hold true, hard substrate may be widely distributed throughout the abyssal depth zone. Data from, for example, the search for flight MH-370 in the Indian Ocean abyss (43), appear to confirm our assumptions. This would help to explain how connectivity between disjunct large seafloor features, such as seamounts and ridges that have so far appeared to be insular and isolated by lack of suitable intermediate habitat, can be maintained.

To further improve our understanding of the biodiversity at the deep seafloor as well as its significant scales—a key goal of marine ecology (44)—abyssal hard rock requires consideration in future research. In the VFZ itself, the populations of endobenthic isopods revealed genetic structure already occurring between stations on either side of the Mid-Atlantic Ridge only a few kilometers apart suggesting population separation at this scale where the topography of the ridge, combined with hydrography, are likely to be the main contributors to the structure (45, 46). The complex landscapes shown by our high-resolution bathymetric maps help to explain these observed genetic patterns. They may play an important role in allopatric

Table 1. Surface area quantification in the VFZ (North Atlantic) by seafloor category and habitat type

Habitat type	Category	Area, km^2	Area, %	Sum (area [%]/habitat type)
Sediment	A1	54,925	58.2	58
Transitional	A2	3,783	4.0	33
	B1	23,120	24.5	
	B2	4,291	4.0	
Hard rock	A3	659	0.7	9
	B3	1,824	1.9	
	C1	3,190	3.4	
	C2	1,423	1.5	
	C3	1,193	1.3	

The total area classified (94,408 km^2) is illustrated in the overview map (Fig. 1). The habitat types are sediment (= low hard-rock exposure potential), transitional (= medium hard-rock exposure potential), and hard rock (= high hard-rock exposure potential).

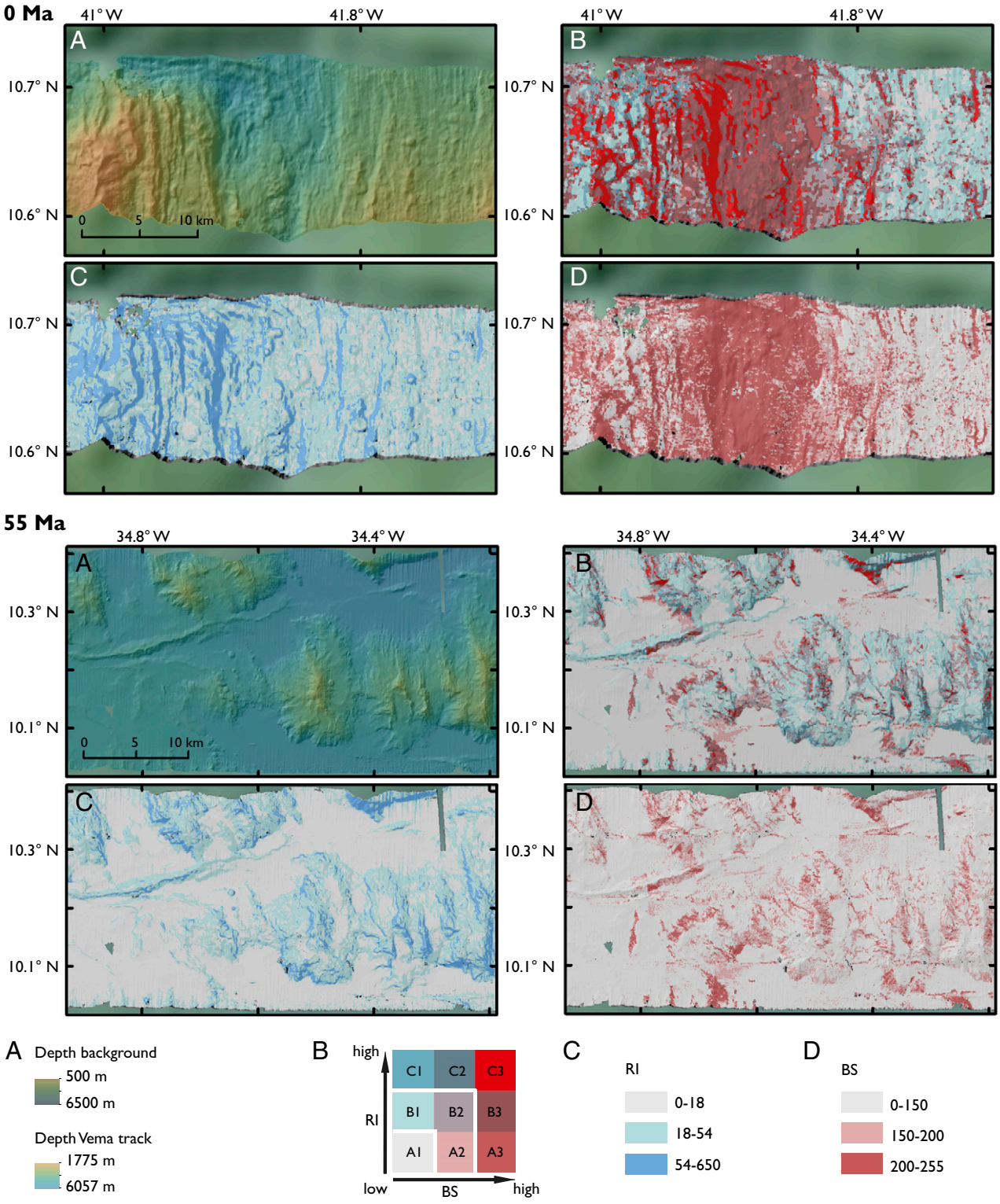

Fig. 2. VFZ (North Atlantic) seafloor at crustal ages of 0 and 55 Ma. (*A*) Bathymetric grid with 60-m resolution. (*B*) Bivariate choropleth map showing the combination of BS and RI. (*C*) Distribution of the RI classes. (*D*) Distribution of BS classes.

speciation, especially in organisms with poor dispersal potential (45). Thorough population-genetic studies in abyssal benthic organisms are still very few (47), yet application of such methods would greatly improve our insight into connectivity and differentiation at the deep seafloor.

Why Only Now? Given the relevance of habitat heterogeneity to explain abyssal biodiversity, it seems difficult to explain why both the rocky habitats themselves as well as their fauna remained principally undetected since the beginning of systematic deep-sea surveys in the 1950s. This is mostly due to undersampling and a

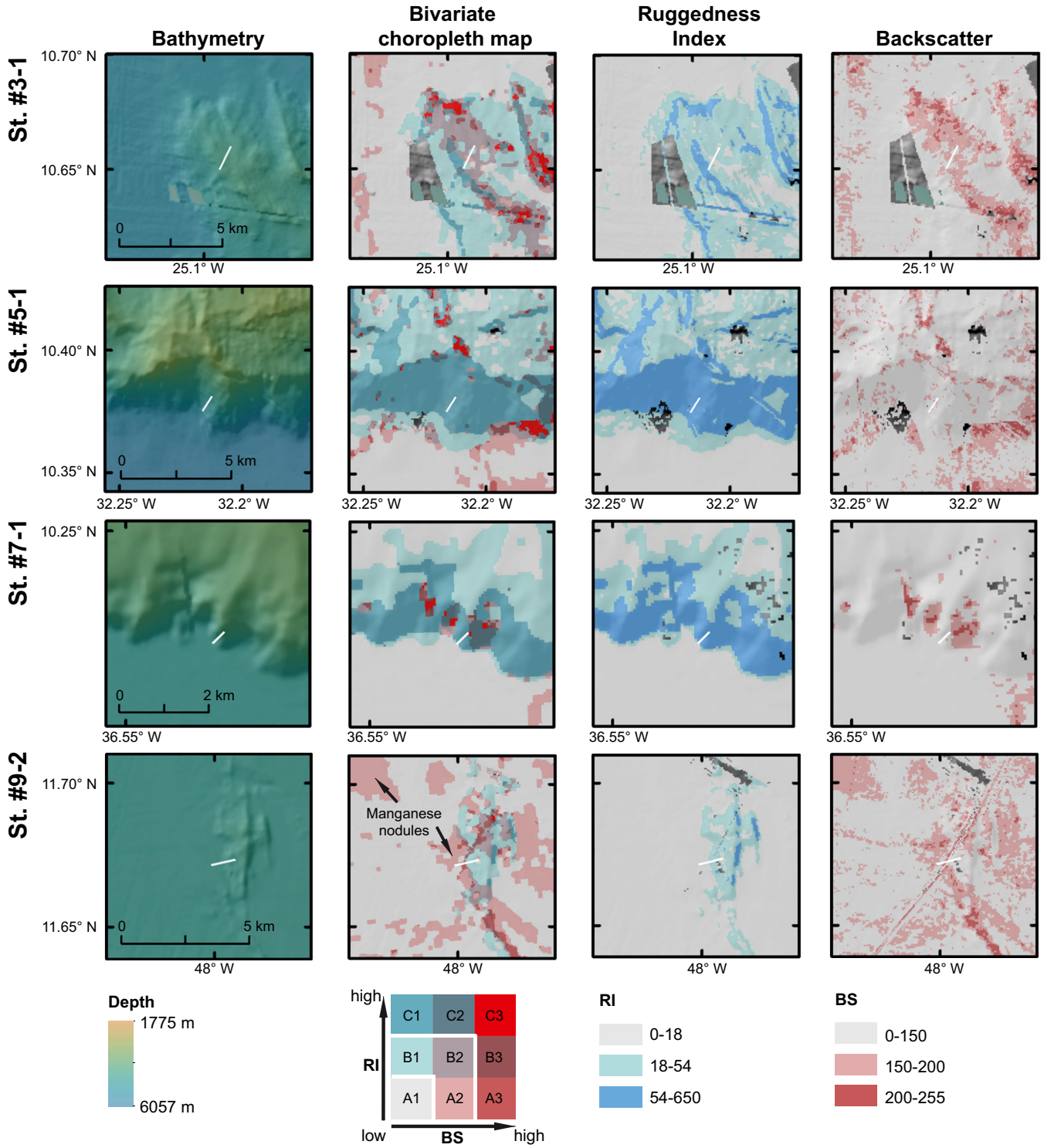

Fig. 3. Habitat characterization at rocky sites in the VFZ (North Atlantic). Hard substrates were recovered from geological rock-dredge stations #3–1, #5–1, and #7–1, as well as C-EBS station #9–2 [see cruise report (37) for photographic evidence]. White bars indicate approximate positions of trawls. The BS column for station (stat.) #5–1 and #7–1 shows that rock catches were successful even where the signal did not suggest the presence of bare rock. BS may therefore underrepresent the available hard substrates and is the more conservative index provided here. Where fresh lava flows or manganese nodules cover the seafloor, the RI may underrepresent the hard-seafloor potential (e.g., stat. #9–2). Points and polygons in various shades of gray represent gaps in the data grid of RI and BS, which has not been interpolated (terrain "hillshade" shining through from below).

paucity of mapping compared to regions on and close to mid-ocean ridges (31, 48), where recent research programs, such as the ECO-MAR (Ecosystems of the Mid-Atlantic Ridge at the Sub-Polar Front and Charlie-Gibbs Fracture Zone) project (30, 33), have greatly advanced this field. Moreover, this is due to a systematic sampling bias. Although some sampling gear has been

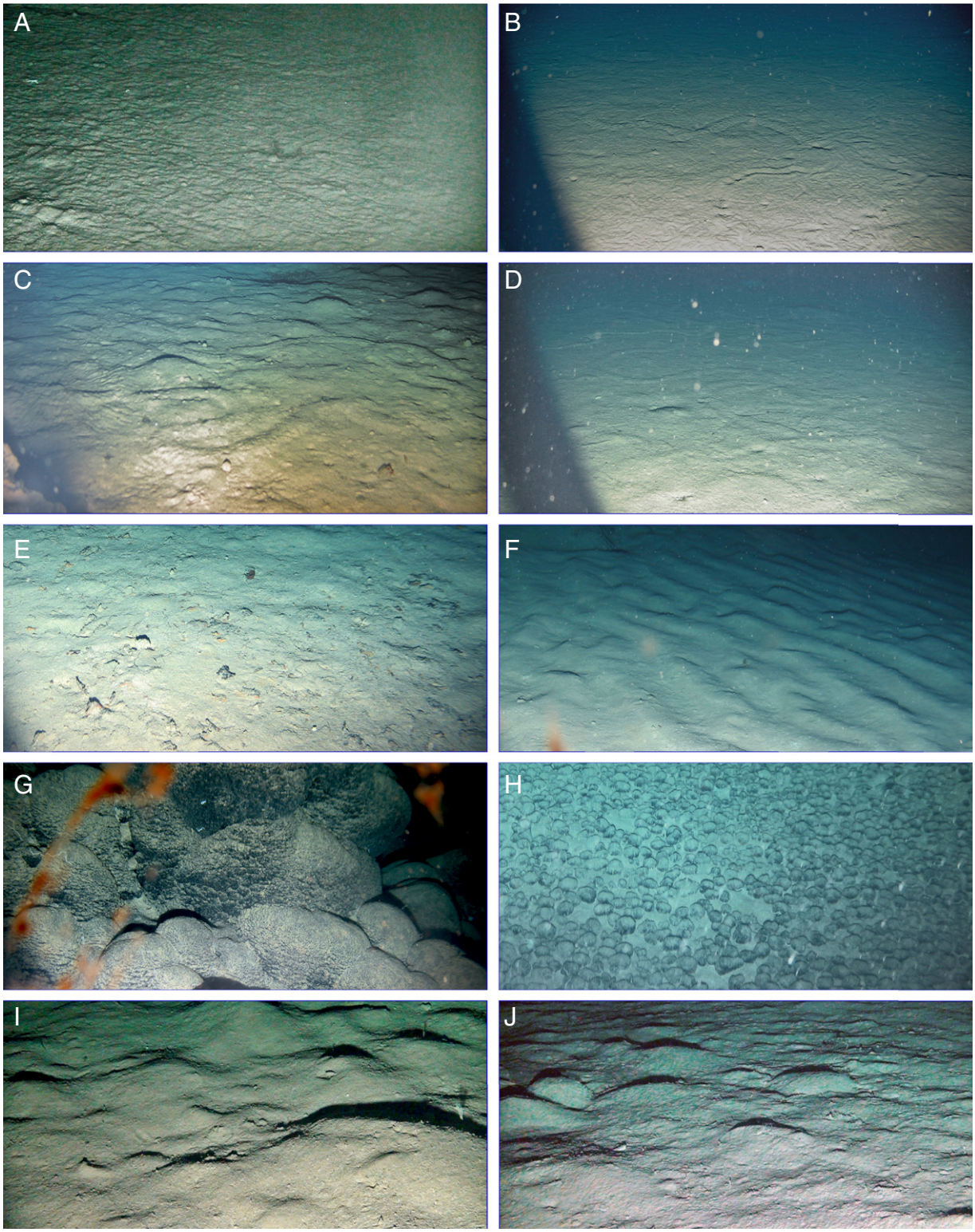

Fig. 4. Seafloor images of the VFZ taken by C-EBS. Approximated habitat classification categories (cat.) are indicated for every image. Scale bar not available due to variation in camera settings and angles. In the following, station numbers of cruise SO237 are indicated in abbreviated fashion. (*A*) Sedimented seafloor with lebensspuren, signs of bioturbation, and *Sargassum* debris, cat. A1, stat. #4–8. (*B*) Sedimented seafloor with lebensspuren, cat. A1, stat. #4–9. (*C*) Sedimented seafloor with lebensspuren, signs of cropping and other bioturbation, burrows and hills, and *Sargassum* debris, cat. A1, stat. #6–8. (*D*) Relatively undisturbed sediment with few life traces and burrows, cat. A2, stat. #8–4. (*E*) Sediment with *Sargassum* debris, traces, and burrows, cat. A1–A2, stat. #9–2. (*F*) Sediment ripples with burrows in the top left, cat. A1–A2, stat. #9–2. (*G*) Manganese crusts, likely cat. A3–B1, stat. #9–2. (*H*) Manganese nodules, cat. A2, stat. #9–2. (*I*) Sediment bumps, cat. A2, stat. #9–8. (*J*) Sediment bumps, tubes, and foraminifera, cat. A1, stat. #11–4. Seafloor images credit: Nils Brenke (photographer).

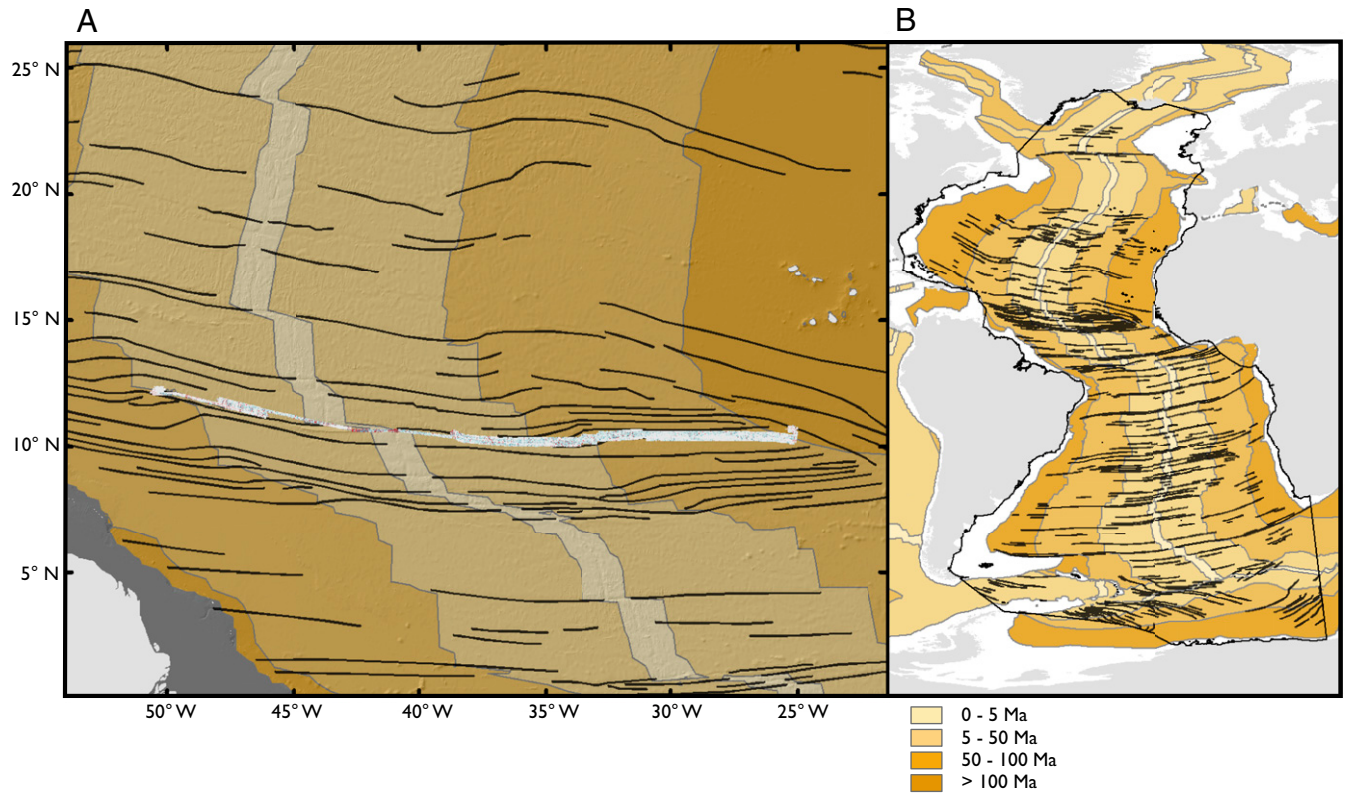

Fig. 5. Distribution of the age classes of the Atlantic Ocean abyssal continental crust and fracture zones. (*A*) Central Atlantic, centered around the VFZ with the bathymetrically surveyed area highlighted and fracture zones indicated by black lines. (*B*) Overview map of the distribution of fracture zones (black lines) in the entire Atlantic Ocean.

specifically designed sufficiently robust to withstand bedrock encounters (e.g., ref. 49), biological seafloor sampling within the abyss is usually restricted to relatively flat sediments for which most biological deep-sea collection devices—namely trawls, grabs, and corers—have been primarily developed (see, e.g., ref. 50). They are preferably not deployed in regions where uneven topography is expected—a decision usually based on The General Bathymetric Chart of the Oceans maps or preparatory hydroacoustic surveys. Nevertheless, if these types of sampling gear encounter hard seafloor, they return empty or damaged. Trawls which may survive encounters with rocky seafloor tend to integrate sampling over a long track, so the contribution to the total sample from hard-substrate fauna may go unrecognized. If a trawl does not survive the encounter with an obstacle it is generally considered a failed station and not reported. To our knowledge, no study has ever specifically targeted abyssal hard-rock fauna aside from manganese nodules, seamounts, and ridges (e.g., refs. 17, 30, 32–34, 42).

Table 2. Quantification of Atlantic fracture-zone seafloor with hard-rock exposure potential

Crustal age, Ma	Hard rock area proportion	Total area, km^2	High-potential area, km^2
0–5	30%	92,709	27,813
5–50	11%	1,583,556	174,191
50–100	5%	1,237,175	61,859
Total		2,913,440	263,863

Estimated proportion and absolute quantity of hard-rock exposure potential available in fracture zones of the Atlantic Ocean, divided by three crustal-age categories.

Outlook. The presented results show that a substantial amount of previously overlooked hard substrate can be expected in the Atlantic Ocean. The introduced methodology serves the purpose of identifying sites for biological and geological sampling. Future sampling programs should prioritize ensuring an integrated geological–biological program and are thus enabled to specifically study the effects of bedrock patches on the abyssal benthos. Key research questions that should be addressed are what impact a heterogeneous abyssal seafloor has on the distribution and connectivity in the benthos populations; if/how environmental gradients associated with hard substrate correlate with species turnover; if abyssal hard-rock patches facilitate connectivity between populations inhabiting supposedly isolated habitats (e.g., seamounts) by acting as dispersal stepping stones; and over what time- and spatial scales, seafloor geological processes impact biological diversity. To achieve this, remotely operated vehicles (ROV) are the gear of choice, enabling sampling at geological settings too risky for the above-mentioned sampling devices. Furthermore, ROV are modular systems that allow integrating a multitude of other aspects of ecosystem studies (various sampler types, photo and video surveys, platform for sensors) (see, e.g., ref. 51). Currently, however, the feasibility of ROV operations is limited by the high associated costs. AUVs may represent suitable alternatives for photographic or hydroacoustic habitat mapping and ground-truthing but their practical applicability is limited by problems with close-to-seafloor navigation in areas with topological relief.

This study is a baseline for the development of multibeam-based habitat assessments at abyssal depths. It highlights the

advantages of taking an integrated and collaborative geological–biological approach to benthic surveys. A better understanding of how abyssal hard-rock patches influence benthic biodiversity will be valuable for species distribution assessment and modeling and may be critical to identify vulnerable marine ecosystems (52), the designation of marine protected areas, and impact assessments connected to deep-sea mining (53).

Materials and Methods

Study Region and Data Acquisition. The Vema Transform Fault forms a large left-lateral offset on the Mid-Atlantic Ridge (MAR) at about 11°N (Fig. 1). Until recently, only the transform region of the VFZ had been mapped and sampled geologically (54–57) and these works indicated that extensive outcrop is exposed at the seafloor in the transform region. The off-axis fracture zones to the east and the west of the MAR are presently almost exclusively known from satellite-measured gravity data (58). Their strong signature on these maps suggested that they are associated with significant seafloor relief exceeding 1,000 m across the VFZ.

For the present work, multibeam bathymetry and BS data collected during the Vema-TRANSIT campaign [German research vessel Sonne cruise SO237 (37, 59, 60)] is evaluated and interpreted (Fig. 1 and *SI Appendix*, Fig. S1) building upon and significantly expanding the scope of a previous publication by Devey et al. (31). Multibeam mapping was performed with the onboard Kongsberg EM 122 multibeam echosounder (Kongsberg Maritime). Data were acquired using SIS acquisition software with equiangular spacing. Sound-velocity profiles were extracted from CTD (instrument measuring conductivity, temperature, and pressure in seawater) data of an AUV and/or the onboard CTD and were updated every 4–6° of longitude along the transect. The EM122 system continuously measures the surface sound velocity and gave no errors during the surveys. This, together with 1) the excellent agreement between our data and data from other vessels in regions where they overlap and 2) the fact that the sedimented fracture zone valley is surveyed as being extremely flat (depth variation <5 m over a 4-km-wide section of the swath—sound-velocity correction problems should lead to concave or convex apparent surfaces) all suggest that the data presented here represent the true seafloor shape. The surveys were conducted with a symmetrical beam spacing of 60° to both sides, a survey speed of 10 kn (18.5 km/h), and a line spacing of 7 NM (13.0 km), giving a typical seafloor swath width of around 9 NM (16.7 km). The interpretation of the acoustic data was confirmed by seafloor sampling and photography (37) using dredges, grabs, gravity corers, a C-EBS, and an AUV (Figs. 3 and 4 and *SI Appendix*, Table S1).

Data Analyses. The QPS Fledermaus Pro software suite (containing the modules DMagic, Fledermaus, and FMGT) was used to postprocess the multibeam data from the VFZ. Besides creating the bathymetric grid, two seafloor parameters were extracted from the multibeam data: ruggedness and BS. BS data represent the acoustic energy that is scattered back to the echosounder after the transmitted sound wave interacted with the seafloor. FMGT was used to apply geometric corrections to the BS values (in decibel) and to normalize them to grayscale values between 0 (black) and 255 (white). The BS mosaic was created with a resolution of 50 m. These relative intensities allow conclusions about the seafloor acoustic reflectivity, a variable related to surface hardness and roughness. Rocky seafloor with little or no sediment cover (e.g., young lava flows, bare basement outcrop) reflects more energy compared to flat, sediment-covered seafloor (61).

Multibeam data were cleaned manually to remove erroneous values and outliers and a bathymetric model at a resolution of 60 m was created. To quantify the ruggedness, the RI was calculated. It is a measure of terrain heterogeneity and represents the mean difference between the measured value of one grid cell (here: water depth in meters) and its surrounding cells (62). The RI was calculated based on the bathymetric model using the software Quantum GIS (QGIS version 2.18.12). No distance weighting and mean of an eight-cell neighborhood of surrounding cells was chosen as input parameters.

Habitat Classification. The defined habitat types "soft sediment" (low hard-rock exposure potential), "transitional/intermediate" (medium hard-rock exposure potential), and hard rock (high hard-rock exposure potential) were differentiated based on the principal assumption that BS intensity and RI are positively correlated with the occurrence of hard seafloor. Locally, sediments accumulate first in depressions and pockets between morphologic highs. The steeper slopes of mounds and ridges act as catchment zones to transport sinking material to the accumulation zones (63) where they form taluses of accumulating sediments (64). The catchment zones themselves stay unsedimented over long times: how long they remain sediment-free depends on slope angles, microruggedness, seismic activity, sedimentation rate, and the intensity of deep-ocean currents.

We defined threshold values for both parameters below which the presence of hard bottom seems unlikely (low potential) and above which exposed hard rock is likely to exist (high potential) in order to make assumptions about the occurrence of hard substrates. These thresholds are ground-truthed by seafloor sampling with geologic rock dredges and EBS (31, 37) (Figs. 3 and 4 and *SI Appendix*, Table S1) as well as seafloor observations (AUV photo surveys).

The combination of the three defined classes (high, medium, and high hard-rock exposure potential) of both parameters (RI and BS) is visualized in a bivariate choropleth map with nine categories. Fig. 2 shows examples of different crustal ages and a variation of BS and RI patterns of the seafloor along the VFZ (*SI Appendix*, Fig. S2).

Based on observations during the cruise, areas with low BS were mainly characterized by values of <150 while high BS areas indicating hard ground, such as, in the best case fresh lava flows (resulting from a strong signal reflection) show values of >200. Therefore, we classified the BS data in values <150 (indicating soft sediments), 150–200 (indicating transition zones as well as poorly sediment-covered seafloor), and >200 (indicating hard ground).

The RI was classified based on Jenks natural breaks classification method that considers clustering within the data. Three classes were created with value ranges between 0–18 m, 18–54 m, and 54–650 m indicating relatively low, medium, and high ruggedness of the terrain, respectively. Increasing RI values correspond to an increasing probability to encounter slopes too steep for long-term sediment accumulation and thus to the occurrence of bare rock. Generally, the friction angle is ∼30° in the marine environment (30, 65), but it is affected by numerous factors, such as grain size, grain shape, and grain packing (66). Gentle slopes of 5°–30° have been reported to be largely sediment-covered with occasional rocky outcrops (30). Slope failure has even been reported at angles as small as 2° (41, 67). However, it is assumed that increasing ruggedness can significantly promote a highly diverse environment including areas with no or low sediment accumulation and areas prone to sediment slumping, in that way allowing the occurrence of bare basement outcrop and hard substrates.

The resulting nine-class bivariate color scheme (Figs. 2 and 3) shows the substrate-category distribution with the rows A–C displaying RI and the columns 1–3 representing BS. Thereby, areas with the lowest BS and RI values fall into field A1 and areas with the highest of both values fall into field C3.

The habitat type soft sediment (category A1) includes flat areas that show low RI and BS signals. The habitat type intermediate/transition (categories A2, B1–B2) features areas that have either a combination of low BS reflection with intermediate RI values, or low to medium RI in combination with medium BS, for instance, resulting from scattered hard-rock patches or manganese nodules. Areas designated with a high hard-seafloor potential (categories A3, B3, C1–C3) are characterized by the occurrence of the high BS class irrespective of ruggedness; regions with low or moderate BS were also considered to have high hard-seafloor potential if they also showed high ruggedness (Fig. 2).

Disagreements between the signals of the two indices can be expected where terrain is highly rugged with steep slopes. In such areas the reflection may get scattered away from the echosounder resulting in low BS intensity. There, RI alone is a good indicator for the presence of high hard-rock exposure potential. Because an accumulation of sediments is rather unlikely there, this combination also falls into the habitat type hard rock (category C1). It is important to note that BS signal depends on the surface angle. The closer the seafloor topography is perpendicular to the direction of sound travel (providing the optimal reflection), the clearer the signal for potentially exposed hard substrate. However, the RI does not suffice to reveal flat, hard-seafloor features where disagreements can be explained with young lava flows (sheet flows) or manganese nodules. Such areas with flat morphologies should have a high BS and a low RI value and accordingly this combination also falls into the hard-rock (category A3) habitat type.

Hard-Rock Availability Estimation for the Atlantic Fracture Zones. Based on a line shapefile defining the location of the Atlantic fracture-zone axes, retrieved from the Global Seafloor Fabric and Magnetic Lineation Database project (type FZ and FZLC) (68), the total area of fracture zones was estimated for the Atlantic Ocean (Fig. 5). Given that for large parts of the Atlantic (and other) fracture zones only crude data of ∼5-km resolution are currently available, the detection of smaller features is difficult. The few available high-resolution maps show Atlantic fracture zones exhibit widths in the range of 6.5–50 km, such as the Romanche Fracture Zone (69). The

proximal Chain Fracture Zone has a width of 20 km over a long distance, but at certain locations narrows down to 5 km and even closes off completely in some areas (69). The Sovanco Fracture Zone in the North Pacific Ocean is 15 km wide (70). Fracture zone width can only be a vague estimation until direct observations provide more details on fracture zone morphology. Therefore for this study a conservative minimum-width estimate of 5 km was assumed for the Atlantic fracture zones, placing a 5-km-wide buffer zone around the fracture-zone lines. It must also be taken into consideration that the vertical relief of fracture zones increases the potential hard-rock area, likely rendering this preliminary assumption of 5-km minimum width an underestimation.

The extent of the Atlantic Ocean was derived from Marine Gazetteer Place Details on marineregions.org (71). Using the 6-min-resolution crustal age grid of Müller et al. (36), the Atlantic seafloor was divided into three age classes (0–5 Ma, 5–50 Ma, 50–100 Ma; Fig. 5). Based on the availability of the distinct habitat types with low, medium, and high hard-rock exposure potential among these age classes in the VFZ, the coverage of these habitat types was estimated for the entire Atlantic fracture zones up to a crustal age of 100 Ma.

Data Availability. The bathymetric dataset has been made available on PANGAEA (https://doi.pangaea.de/10.1594/PANGAEA.893352) (72).

ACKNOWLEDGMENTS. The captain and crew of RV Sonne are acknowledged for a great job during SO237. The authors are thankful for helpful suggestions and comments by various members of T.R.'s and A.B.'s previous Hamburg University working group and current laboratory, as well as for critical feedback by Jörn Thiede, who significantly helped to improve this manuscript. Article processing and open access fees have been covered by a fellowship from the Johanna Quandt Young Academy at Goethe University to T.R. The project was undertaken with financial support of the BMBF (German Ministry for Science and Education), Grant 03G0227A.

1. E. Ramirez-Llodra *et al*., Deep, diverse and definitely different: Unique attributes of the world's largest ecosystem. *Biogeosciences* **7**, 2851–2899 (2010).
2. L. Watling, J. Guinotte, M. R. Clark, C. R. Smith, A proposed biogeography of the deep ocean floor. *Prog. Oceanogr.* **111**, 91–112 (2013).
3. C. R. Smith, F. C. De Leo, A. F. Bernardino, A. K. Sweetman, P. M. Arbizu, Abyssal food limitation, ecosystem structure and climate change. *Trends Ecol. Evol.* **23**, 518–528 (2008).
4. D. Thistle, "The deep-sea floor: An overview" in *Ecosystems of the Deep Ocean, Ecosystems of the World*, P. A. Tyler, Ed. (Elsevier Science, Amsterdam, 2003), pp. 5–38.
5. P. T. Harris, M. Macmillan-Lawler, J. Rupp, E. K. Baker, Geomorphology of the oceans. *Mar. Geol.* **352**, 4–24 (2014).
6. D. Voelker, "Abyssal Plains" in *Encyclopedia of Marine Geosciences*, J. Harff, M. Meschede, S. Petersen, J. Thiede, Eds. (Springer Reference, 2016), pp. 1–5.
7. J. D. Gage, P. A. Tyler, *Deep-Sea Biology: A Natural History of Organisms at the Deep-Sea Floor*, (Cambridge University Press, 1991).
8. J. M. Whittaker, A. Goncharov, S. E. Williams, R. D. Müller, G. Leitchenkov, Global sediment thickness data set updated for the Australian-Antarctic Southern Ocean. *Geochem. Geophys. Geosyst.* **14**, 3297–3305 (2013).
9. D. L. Divins, "Total Sediment Thickness of the World's Oceans and Marginal Seas" NOAA National Geophysical Data Center. https://www.ngdc.noaa.gov/mgg/sedthick/sedthick.html. Accessed 1 June 2020.
10. D. K. Rea *et al*., Broad region of no sediment in the southwest Pacific Basin. *Geology* **34**, 873–876 (2006).
11. G. P. Glasby, Broad region of no sediment in the southwest Pacific basin: Comment and reply comment. *Geology* **35**, e132 (2007).
12. D. K. Rea, M. W. Lyle, Broad region of no sediment in the southwest Pacific Basin: Comment and reply reply. *Geology* **35**, e133 (2007).
13. E. E. Cordes *et al*., The influence of geological, geochemical, and biogenic habitat heterogeneity on seep biodiversity. *Mar. Ecol.* **31**, 51–65 (2010).
14. L. A. Levin, M. Sibuet, A. J. Gooday, C. R. Smith, A. Vanreusel, The roles of habitat heterogeneity in generating and maintaining biodiversity on continental margins: An introduction. *Mar. Ecol.* **31**, 1–5 (2010).
15. A. Stein, K. Gerstner, H. Kreft, Environmental heterogeneity as a universal driver of species richness across taxa, biomes and spatial scales. *Ecol. Lett.* **17**, 866–880 (2014).
16. J. M. Durden, B. J. Bett, D. O. B. Jones, V. A. I. Huvenne, H. A. Ruhl, Abyssal hills – hidden source of increased habitat heterogeneity, benthic megafaunal biomass and diversity in the deep sea. *Prog. Oceanogr.* **137**, 209–218 (2015).
17. E. Simon-Lledó *et al*., Megafaunal variation in the abyssal landscape of the Clarion Clipperton zone. *Prog. Oceanogr.* **170**, 119–133, 10.1016/j.pocean.2018.11.003 (2019).
18. A. Vanreusel *et al*., The contribution of deep-sea macrohabitat heterogeneity to global nematode diversity. *Mar. Ecol.* **31**, 6–20 (2010).
19. S. N. C. Woolley *et al*., Deep-sea diversity patterns are shaped by energy availability. *Nature* **533**, 393–396 (2016).
20. M. Yasuhara, R. Danovaro, Temperature impacts on deep-sea biodiversity. *Biol. Rev.* **91**, 275–287, 10.1111/brv.12169/full (2016).
21. O. S. Ashford, A. J. Kenny, C. R. S. Barrio Froján, T. Horton, A. D. Rogers, Investigating the environmental drivers of deep-seafloor biodiversity: A case study of peracarid crustacean assemblages in the Northwest Atlantic Ocean. *Ecol. Evol.* **9**, 14167–14204 (2019).
22. L. A. Levin, P. K. Dayton, Ecological theory and continental margins: Where shallow meets deep. *Trends Ecol. Evol.* **24**, 606–617 (2009).
23. L. A. Levin *et al*., Environmental influences on regional deep-sea species diversity. *Annu. Rev. Ecol. Syst.* **32**, 51–93 (2001).
24. O. David, C. Lannou, H. Monod, J. Papaïx, D. Traore, Adaptive diversification in heterogeneous environments. *Theor. Popul. Biol.* **114**, 1–9 (2017).
25. R. Mazzucco, M. Doebeli, U. Dieckmann, The influence of habitat boundaries on evolutionary branching along environmental gradients. *Evol. Ecol.* **32**, 563–585 (2018).
26. A. Brandt *et al*., First insights into the biodiversity and biogeography of the Southern Ocean deep sea. *Nature* **447**, 307–311 (2007).
27. J. D. Gage, "High benthic species diversity in deep-sea sediments: The importance of hydrodynamics" in *Marine Biodiversity: Patterns and Processes*, R. P. G. Ormond, J. D. Gage, M. V. Angel, Eds. (Cambridge University Press, 1997), pp. 148–177.
28. H. L. Sanders, Marine benthic diversity: A comparative study. *Am. Nat.* **102**, 243–282 (1968).
29. P. V. R. Snelgrove, C. R. Smith, A riot of species in an environmental calm: The paradox of the species-rich deep-sea floor. *Oceanogr. Mar. Biol. Annu. Rev.* **40**, 311–342 (2002).
30. I. G. Priede *et al*., Does presence of a mid-ocean ridge enhance biomass and biodiversity? *PLoS One* **8**, e61550 (2013).
31. C. W. Devey *et al*., Habitat characterization of the Vema fracture zone and Puerto Rico trench. *Deep Sea Res. Part II Top. Stud. Oceanogr.* **148**, 7–20 (2018).
32. A. Purser *et al*., Association of deep-sea incirrate octopods with manganese crusts and nodule fields in the Pacific Ocean. *Curr. Biol.* **26**, R1268–R1269 (2016).
33. T. Niedzielski, Å. Høines, M. A. Shields, T. D. Linley, I. G. Priede, A multi-scale investigation into seafloor topography of the northern Mid-Atlantic Ridge based on geographic information system analysis. *Deep Sea Res. Part II Top. Stud. Oceanogr.* **98**, 231–243 (2013).
34. A. Vanreusel, A. Hilario, P. A. Ribeiro, L. Menot, P. M. Arbizu, Threatened by mining, polymetallic nodules are required to preserve abyssal epifauna. *Sci. Rep.* **6**, 26808 (2016).
35. P. A. Tyler, M. Baker, E. Ramirez Llodra, "Deep-sea benthic habitats" in *Biological Sampling in the Deep Sea*, M. R. Clark, M. Consalvey, A. A. Rowden, Eds. (Wiley-Blackwell, 2016), pp. 1–15.
36. R. D. Müller, M. Sdrolias, C. Gaina, W. R. Roest, Age, spreading rates, and spreading asymmetry of the world's ocean crust. *Geochem. Geophys. Geosyst.* **9**, Q04006 (2008).
37. C. W. Devey, RV SONNE Fahrtbericht/Cruise Report SO237 Vema-TRANSIT. *Geomar Rep.* **23**, 130 (2015).
38. A. Brandt *et al*., Epifauna of the Sea of Japan collected via a new epibenthic sledge equipped with camera and environmental sensor systems. *Deep Sea Res. Part II Top. Stud. Oceanogr.* **86–87**, 43–55 (2013).
39. L. Mayer *et al*., The Nippon Foundation—GEBCO seabed 2030 project: The quest to see the world's oceans completely mapped by 2030. *Geosciences* **8**, 63 (2018).
40. C. R. McClain, J. P. Barry, Habitat heterogeneity, disturbance, and productivity work in concert to regulate biodiversity in deep submarine canyons. *Ecology* **91**, 964–976 (2010).
41. C. R. Smith, A. W. J. Demopoulos, "Ecology of the deep Pacific Ocean floor" in *Ecosystems of the Deep Ocean, Ecosystems of the World*, P. A. Tyler, Ed. (Elsevier, 2003), pp. 179–218.
42. D. J. Amon *et al*., Insights into the abundance and diversity of abyssal megafauna in a polymetallic-nodule region in the eastern Clarion-Clipperton Zone. *Sci. Rep.* **6**, 30492 (2016).
43. Geoscience Australia, MH370—Phase One Data Release (2017). http://www.ga.gov.au/about/projects/marine/mh370-data-release. Accessed 1 June 2020.
44. D. Zeppilli, A. Pusceddu, F. Trincardi, R. Danovaro, Seafloor heterogeneity influences the biodiversity-ecosystem functioning relationships in the deep sea. *Sci. Rep.* **6**, 26352 (2016).
45. S. Bober, S. Brix, T. Riehl, M. Schwentner, A. Brandt, Does the Mid-Atlantic Ridge affect the distribution of abyssal benthic crustaceans across the Atlantic Ocean? *Deep Sea Res. Part II Top. Stud. Oceanogr.* **148**, 91–104 (2018).
46. T. Riehl, L. Lins, A. Brandt, The effects of depth, distance, and the Mid-Atlantic Ridge on genetic differentiation of abyssal and hadal isopods (Macrostylidae). *Deep Sea Res. Part II Top. Stud. Oceanogr.* **148**, 74–90 (2018).
47. M. L. Taylor, C. N. Roterman, Invertebrate population genetics across Earth's largest habitat: The deep-sea floor. *Mol. Ecol.* **26**, 4872–4896 (2017).
48. A. Brandt *et al*., Challenges of deep-sea biodiversity assessments in the Southern Ocean. *Adv. Polar Sci.* **25**, 204–212 (2014).
49. N. Brenke, An epibenthic sledge for operations on marine soft bottom and bedrock. *Mar. Technol. Soc. J.* **39**, 10–21 (2005).
50. M. R. Clark, M. Consalvey, A. A. Rowden, Eds., *Biological Sampling in the Deep Sea*, (Wiley-Blackwell, 2016).
51. I. G. Priede *et al*., The ECO-MAR (ecosystem of the Mid-Atlantic Ridge at the sub-polar front and Charlie Gibbs fracture zone) project: Description of the benthic sampling programme 2007–2010. *Mar. Biol. Res.* **9**, 624–628 (2013).
52. A. M. Rengstorf, C. Mohn, C. Brown, M. S. Wisz, A. J. Grehan, Predicting the distribution of deep-sea vulnerable marine ecosystems using high-resolution data: Considerations and novel approaches. *Deep Sea Res. Part Oceanogr. Res. Pap.* **93**, 72–82 (2014).

53. V. Tilot, R. Ormond, J. Moreno Navas, T. S. Catalá, The benthic megafaunal assemblages of the CCZ (Eastern Pacific) and an approach to their management in the face of threatened anthropogenic impacts. *Front. Mar. Sci.* **5**, 1–25, 10.3389/fmars.2018.00007 (2018).
54. M. Cannat *et al*., A geological cross-section of the Vema fracture zone transverse ridge, Atlantic ocean. *J. Geodyn.* **13**, 97–117 (1991).
55. M. Cannat, M. Seyler, Transform tectonics, metamorphic plagioclase and amphibolitization in ultramafic rocks of the Vema transform fault (Atlantic Ocean). *Earth Planet. Sci. Lett.* **133**, 283–298 (1995).
56. A. Cipriani, E. Bonatti, D. Brunelli, M. Ligi, 26 million years of mantle upwelling below a segment of the Mid Atlantic Ridge: The Vema lithospheric section revisited. *Earth Planet. Sci. Lett.* **285**, 87–95 (2009).
57. Y. Lagabrielle *et al*., Vema Fracture Zone (central Atlantic): Tectonic and magmatic evolution of the median ridge and the eastern ridge-Transform intersection domain. *J. Geophys. Res. Solid Earth* **97**, 17331–17351 (1992).
58. W. H. Smith, D. T. Sandwell, Global sea floor topography from satellite altimetry and ship depth soundings. *Science* **277**, 1956–1962 (1997).
59. T. Riehl, S. Kaiser, A. Brandt, Vema-TRANSIT—An interdisciplinary study on the bathymetry of the Vema-fracture zone and Puerto Rico TRench as well as Abyssal AtlaNtic BiodiverSITy. *Deep Sea Res. Part II Top. Stud. Oceanogr.* **148**, 1–6 (2018).
60. C. W. Devey, N. Augustin, I. A. Yeo, Raw multibeam EM122 data and data products: SONNE cruise SO237 (North Atlantic). PANGEA. https://doi.org/10.1594/PANGAEA.893352. Accessed 1 June 2020.
61. A. Hewitt, R. Salisbury, J. Wilson, Using multibeam echosounder backscatter to characterize seafloor features. *Sea Technol.* **51**, 10–13 (2010).
62. S. J. Riley, A terrain ruggedness index that quantifies topographic heterogeneity. *Intermt. J. Sci.* **5**, 23–27 (1999).
63. N. C. Mitchell, Diffusion transport model for pelagic sediments. *J. Geophys. Res.* **100**, 19–991 (1995).
64. I. G. Priede *et al*., The ecosystem of the Mid-Atlantic Ridge at the sub-polar front and Charlie–Gibbs Fracture Zone; ECO-MAR project strategy and description of the sampling programme 2007–2010. *Deep Sea Res. Part II Top. Stud. Oceanogr.* **98**, 220–230 (2013).
65. H. G. Brandes, Geotechnical characteristics of deep-sea sediments from the North Atlantic and North Pacific oceans. *Ocean Eng.* **38**, 835–848 (2011).
66. J. W. Kirchner, W. E. Dietrich, F. Iseya, H. Ikeda, The variability of critical shear stress, friction angle, and grain protrusion in water-worked sediments. *Sedimentology* **37**, 647–672 (1990).
67. M. Urlaub, P. J. Talling, A. Zervos, D. Masson, What causes large submarine landslides on low gradient (< 2°) continental slopes with slow (0.15 m/kyr) sediment accumulation? *J. Geophys. Res. Solid Earth* **120**, 6722–6739 (2015).
68. K. J. Matthews, R. D. Müller, P. Wessel, J. M. Whittaker, The tectonic fabric of the ocean basins. *J. Geophys. Res. Solid Earth* **116**, B12109 (2011).
69. H. Mercier, K. G. Speer, J. Honnorez, Flow pathways of bottom water through the Romanche and Chain fracture zones. *Deep Sea Res. Part Oceanogr. Res. Pap.* **41**, 1457–1477 (1994).
70. D. S. Cowan, M. Botros, H. P. Johnson, Bookshelf tectonics: Rotated crustal blocks within the Sovanco fracture zone. *Geophys. Res. Lett.* **13**, 995–998 (1986).
71. International Hydrographic Organization, Limits of Oceans and Seas, 3rd Ed. (International Hydrographic Organization Special Publication No. 23, 1953).
72. C. W. Devey, N. Augustin, I. A. Yeo, Raw multibeam EM122 data and data products: SONNE cruise SO237 (North Atlantic). PANGEA. https://doi.org/10.1594/PANGAEA.893352. Accessed 1 June 2020.